

## Critical properties of pure and randomly dilute dysprosium aluminum garnet

J. M. Hastings, L. M. Corliss, and W. Kunnmann

*Chemistry Department, Brookhaven National Laboratory, Upton, New York 11973*

(Received 12 September 1984)

Critical properties of the Ising antiferromagnet, dysprosium aluminum garnet (DAG), have been studied by neutron scattering techniques in polycrystalline specimens of the pure compound and in samples containing 1 at. % and 5 at. % yttrium substituted for dysprosium. All samples were prepared by a precipitation technique to ensure homogeneously random yttrium substitution. Critical indices and amplitudes for pure DAG showed satisfactory agreement with theory, lending confidence in the powder method and suggesting that the anomalously low value of  $\beta$  obtained with single crystals may have been caused by extinction. In the case of the diluted samples, the value of  $\beta$  increased as expected on the basis of recent calculations of Newman and Riedel. However, the temperature dependence of the correlation range parameter exhibited an anomaly for which there is at present no explanation applicable to an Ising system: The range parameter remained essentially "infinite" between  $T_N$  and an "upper critical temperature," above which it exhibited a normal power-law decrease.

### I. INTRODUCTION

Randomly dilute three-dimensional (3D) Ising magnets have been the subject of a number of experimental and theoretical investigations in recent years. Much of this interest was generated by a suggestion by Harris<sup>1</sup> that the critical behavior of  $n$ -vector models would be unaltered by the addition of a small concentration of impurities if the heat-capacity exponent  $\alpha$  were negative, but would exhibit a crossover to a new critical behavior if, as in the case of the 3D Ising model,  $\alpha$  were positive. These conclusions were subsequently confirmed by renormalization-group calculations.<sup>2,3</sup>

Early attempts to distinguish by means of neutron scattering between the properties of the pure 3D Ising model and those of the random system were inconclusive. In the case of Mn/ZnF<sub>2</sub> studied by Meyer and Dietrich,<sup>4</sup> as well as in that of Co/ZnF<sub>2</sub> investigated by Cowley and Carneiro,<sup>5</sup> accuracy was severely limited by a smearing of the transition caused by gradients in chemical composition. Dunlap and Gottlieb,<sup>6</sup> however, in an NMR study of Mn<sub>0.864</sub>Zn<sub>0.136</sub>F<sub>2</sub>, reported a sharp transition and a value of  $\beta$  agreeing closely with the predicted value of Newman and Riedel<sup>3</sup> for the random 3D Ising model. More recently, a highly diluted system Fe<sub>1-x</sub>Zn<sub>x</sub>F<sub>2</sub> with  $x=0.4$  and  $0.5$  was studied by Birgeneau *et al.*<sup>7</sup> using both neutron scattering and birefringence measurements. The effect of smearing was limited in the neutron measurements by masking the crystal to expose a reasonably homogeneous region, and in the birefringence measurements, by orienting the laser beam perpendicular to the concentration gradient. The measured indices  $\gamma$ ,  $\nu$ , and  $\alpha$  were found to be consistent with the theoretical predictions of Newman and Riedel<sup>3</sup> for the random-exchange Ising model. The temperature dependence of the order parameter was not measured in these experiments because the crystal was found to suffer from extreme extinction.

However, taken together with the measurement of  $\beta$  by Dunlap and Gottlieb<sup>6</sup> they indicate that random-Ising theory gives a good account of critical behavior of site-diluted Ising-type iron-group fluorides.

Because of the importance of the ideas involved, it was thought desirable to investigate the effect of random substitution in a different structure type. Dysprosium aluminum garnet (DAG), the well-characterized<sup>8,9</sup> cubic non-collinear Ising antiferromagnet, was selected for this purpose. To avoid gradients in composition that inevitably arise in single-crystal solid solutions, it was decided to utilize polycrystalline specimens which could be prepared by co-precipitation, thus ensuring a homogeneously random product. The present experiment was restricted to the region of small randomness to which current theory most closely applies. To explore this region, samples containing 1 and 5 at. % of nonmagnetic yttrium were studied and compared to pure polycrystalline DAG.

The use of powders does have obvious disadvantages: Intensities are considerably lower and resolution is poorer than with single crystals. In addition, powder averaging over a comparatively large range of wave-vector transfers makes it more difficult to satisfy the quasielastic approximation. To further complicate matters in the case of DAG, the absorption is so high that sample thickness has to be reduced to  $\sim 1$  mm. On the other hand, the advantage of the powder method, and one that will prove to be of considerable significance in DAG, is the avoidance of extinction. Single-crystal studies<sup>9</sup> of pure DAG have given a value of  $\beta$  of  $0.26 \pm 0.02$ , approximately 20% lower than the theoretical value. Although internal evidence of the experiment indicated the absence of secondary extinction, it is by no means certain that the low value of  $\beta$  was not in fact attributable to the very high state of perfection of the single crystals. An additional objective of the powder experiment was to redetermine  $\beta$  under conditions where extinction is clearly absent.

## II. SAMPLE PREPARATION

Synthesis of single-phase garnet powders with correct stoichiometry and a random distribution of yttrium on dysprosium sites was carried out by means of a combination of wet- and solid-state chemistry methods which ensured good reproducibility in the conditions of preparation of the various samples. The starting materials were spectroscopically pure  $Y_2O_3$  and  $Dy_2O_3$ , repurified by firing in a hydrogen atmosphere at  $800^\circ C$  for several hours, highest-grade aluminum metal, surface cleaned with concentrated KOH solution, and reagent-grade aqueous HBr and  $NH_4OH$ .

Two stock solutions containing the equivalents of known concentrations of  $Y_3Al_5O_{12}$  and  $Dy_3Al_5O_{12}$  were prepared by dissolving the appropriate amount of oxide and aluminum metal in a minimum amount of concentrated HBr. Aliquot portions of these solutions were used in the synthesis of *all* samples. (HBr was used instead of HCl because of the difficulty of removing any oxychlorides in the product as opposed to oxybromides.) Hydrated oxides were rapidly co-precipitated by titrating mixtures of these solutions with 1:1  $NH_4OH$  until neutrality was reached. After overnight digestion, the co-precipitated oxides were oven-dried, ground to a fine dust, fired in air at  $1200^\circ C$  for several days, cooled, reground, and refired. To make sure that the precipitated oxides contained the calculated amounts of the metals, the filtrate was analyzed for trace amounts, by means of x-ray fluorescence, and found to contain only negligible residues.

## III. CRITICAL SCATTERING FROM A POWDER

When viewed in reciprocal space, the critical scattering from a polycrystalline specimen arises from a spherical shell whose radius,  $r$ , is the reciprocal of the  $d$  spacing of the magnetic reflection being studied. The critical scattering can be measured by moving the point of observation, determined by the angle between the incident and scattered beams, radially through this spherical shell. The quasielastic approximation is well satisfied in DAG (Ref. 8) and thus the scattering,  $d\chi$ , associated with an element of surface of the sphere can be taken to be Lorentzian:

$$d\chi = \frac{A}{\kappa^2 + q^2} d\sigma,$$

where  $q$  is the distance from the surface element  $d\sigma$  to the point of observation, and  $\kappa$  is the inverse range parameters. For the case of perfect resolution, the total intensity at a point a distance  $q_0$  from a shell of radius  $r$  (see Fig. 1) is given by

$$\begin{aligned} \chi(q_0) &= 2\pi d^2 \int_0^\pi \frac{A}{\kappa^2 + q^2} \sin\theta d\theta \\ &= \frac{\pi r}{r + q_0} \ln \left[ 1 + \frac{4r(r + q_0)}{\kappa^2 + q_0^2} \right]. \end{aligned} \quad (1)$$

For finite resolution, this result must be convoluted with the instrumental resolution function, which is an ellipsoid centered at  $q_0$ , with coordinates that can be taken

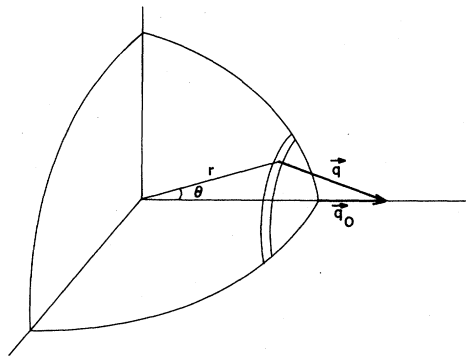


FIG. 1. Representation in reciprocal space of critical scattering from a polycrystalline specimen for the case of perfect resolution. The source of scattering is a spherical surface of radius  $r$ , the reciprocal of the  $d$  spacing of the magnetic reflection. The point of observation is the end point of the vector  $q_0$  and the experimental scan is obtained by varying  $q_0$  along a radial direction.

parallel and perpendicular to the direction of scan,  $q_0$ . By symmetry, the intensity of scattering is constant on planes through the resolution ellipsoid perpendicular to  $q_0$ , and thus the convolution is effectively one dimensional.

Figure 2 shows a typical scan of intensity as a function of  $q_0$  for pure DAG powder, through the position corresponding to the (110) magnetic reflection, at a temperature above  $T_N$ . The solid line is a least-squares fit of the data to the convolution of the cross section (1) with the instrumental resolution function. Below  $T_N$ , this type of scan results in a superposition of Bragg scattering and critical scattering. In the present work the two have been separated by first fitting the wings of the scan, outside the range of Bragg scattering, to obtain the critical scattering, and then subtracting the calculated critical scattering at

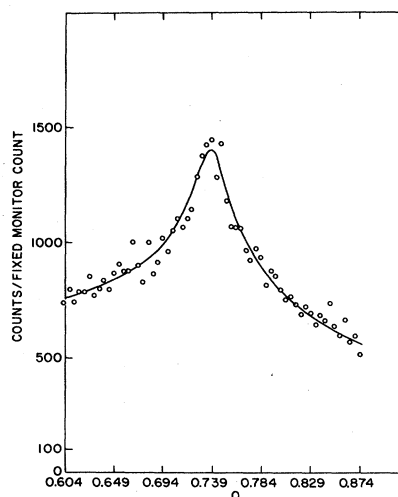


FIG. 2. Typical critical scattering scan for pure DAG at  $T = 2.562$  K. The scan variable  $Q$  is measured from the origin of reciprocal space. The curve through the points is a least-squares fit to the data of the convolution of Eq. (1) with the experimental resolution function, and corresponds to a value of  $\kappa$  of  $0.00519 \text{ \AA}^{-1}$ .

the center to obtain the Bragg component. Correction of the Bragg peak for overlapping critical scattering is most important near  $T_N$ . In single crystals the separation is aided by the sharpness of the Bragg reflection; in powders, by the relative flatness of the critical scattering.

#### IV. DETERMINATION OF $T_N$

It is generally recognized that if data are restricted to the region close to  $T_N$ , the values of critical indices obtained from log-log plots of the limiting behavior are strongly coupled to  $T_N$  itself. One way to obtain an independent measure of  $T_N$  under the conditions of the actual experiment is to determine the temperature at which the critical scattering peaks, by measuring the intensity just outside the angular range corresponding to Bragg scattering. This method frequently lacks sensitivity in single crystals and is even more insensitive in powder work. Another procedure is to choose that value which gives a satisfactory fit to the temperature dependence of both the order parameter below  $T_N$  and the critical scattering above. This method, as we shall see, is also not suited to the present experiment.

One method that has been found satisfactory involves determining the extent of agreement between the observed scan and that calculated for critical scattering alone, with  $\kappa=0$ , and a normalization constant obtained from fits at higher temperatures. Since the shape is distorted by the appearance of Bragg scattering,  $T_N$  can be taken as the point where the agreement factor changes abruptly as the temperature of the scan is varied. This procedure is illustrated in Fig. 3 for the case of 5-at. % sample. A second, and related method is to subtract from the Bragg peak that part of the calculated critical scattering for  $\kappa=0$  that falls within the Bragg scattering angular range. This difference will be negative above  $T_N$ , where  $\kappa$  is greater

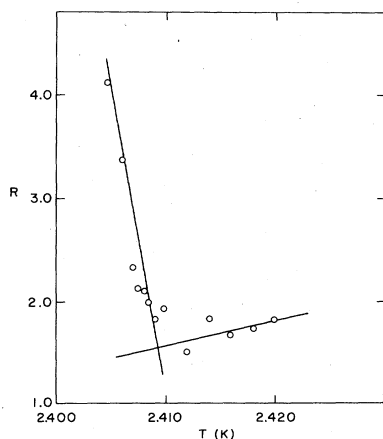


FIG. 3. Temperature variation of the agreement factor,  $R$ , characterizing the least-squares fit to the experimental scan by the theoretical expression for  $\kappa=0$ . The Néel temperature corresponds to the point where  $R$  rises abruptly because of the onset of Bragg scattering. Data are for the 5-at. % sample.

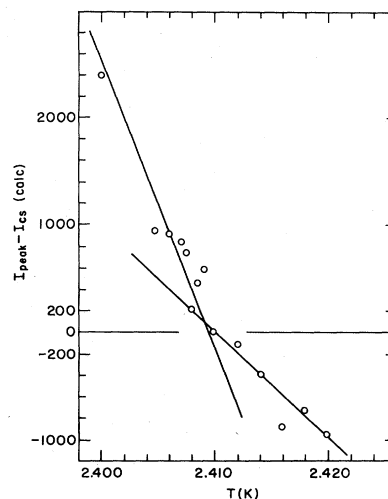


FIG. 4. Temperature variation of the difference between the integrated intensity in the angular range of the Bragg peak, and that calculated for the critical scattering in the same interval with  $\kappa=0$ . The Néel point corresponds to zero difference. Data are for the 5-at. % sample.

than zero, positive below, because of the Bragg scattering, and zero at the critical point. Figure 4 illustrates this procedure for the 5-at. % sample. The combined accuracy of the two methods is estimated to be  $\pm 0.5$  mK or 0.02%. In addition to providing a "physical" measure of  $T_N$ , the methods demonstrate that the transition in the diluted sample is indeed sharp, as expected for the 3D Ising model. The success of these procedures clearly depends on the applicability of the Lorentzian approximation. In the present instance, it had been found to hold for all samples over the whole temperature range above  $T_N$ .

#### V. PURE DAG

Measurements were first undertaken with pure DAG in order to establish the validity of the powder method and

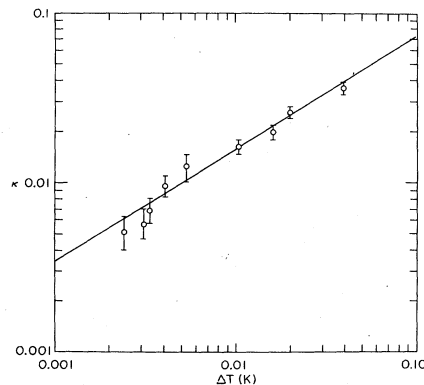


FIG. 5. Power-law fit of the temperature dependence of the inverse range parameter  $\kappa$  in the disordered phase for pure DAG.

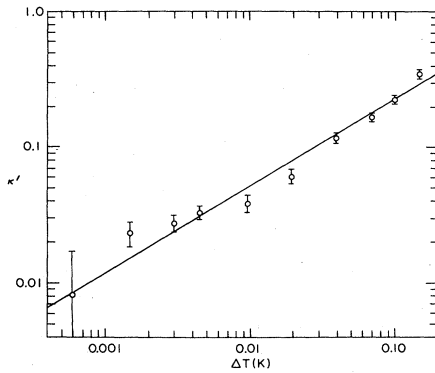


FIG. 6. Power-law fit of the temperature dependence of the inverse range parameter  $\kappa'$  in the ordered phase for pure DAG.

to provide a basis of comparison of pure and site-diluted samples. Earlier studies<sup>9</sup> of pure DAG single crystals gave an anomalously low value for the magnetization index  $\beta$  ( $0.26 \pm 0.02$ ), whereas the critical scattering behaved as expected. Later unpublished experiments with different crystals confirmed the earlier findings and raised the suspicion that the low value was caused by extinction. This possibility had been suggested in the original work but was not seriously entertained because weaker higher-order magnetic reflections gave the same value of  $\beta$ . Nuclear reflections studied in that investigation showed no trend in the calculated-to-observed ratios with the level of intensity, but nevertheless anomalies were present suggesting high effective absorption in the interior of the crystal. Extinction effects should be inconsequential in measurements on fine powders and thus the present experiment would be expected to clarify this issue.

The temperature dependence of the inverse range parameter  $\kappa$  is shown in the log-log plot of Fig. 5. Values of the corresponding parameter  $\kappa'$  for temperatures below  $T_N$  were obtained by fitting the critical scattering in the regions outside the angular range in which the Bragg scattering occurs, and are shown in Fig. 6. A similar plot of the integrated Bragg intensity, corrected for critical scattering under the peak, gives  $2\beta$  and is shown in Fig. 7.

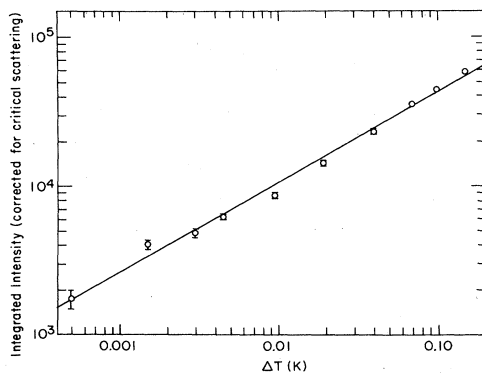


FIG. 7. Power-law fit of the temperature dependence of the magnetic Bragg intensity for pure DAG.

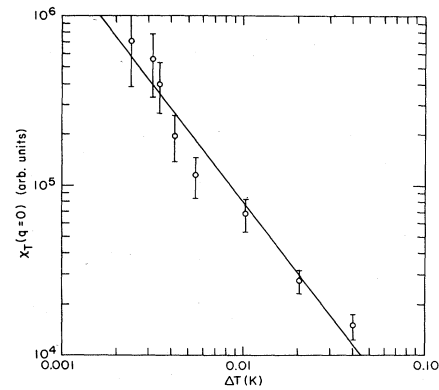


FIG. 8. Power-law fit of the temperature dependence of the staggered susceptibility  $\chi_T(q=0)$  for pure DAG.

Finally, the derived staggered susceptibility  $\chi_T(q=0)$  is given in Fig. 8.

Critical exponents and amplitudes are collected in Table I. The major source of error in the exponents comes from the uncertainty in  $T_N$  and the errors quoted in the table are based on the results of fitting with different values of  $T_N$ , rather than on the least-squares error for the best value of  $T_N$ , which is much smaller.

The agreement between theory and experiment for pure DAG powder is clearly acceptable and indicates that the experimental procedures and method of analysis are satisfactory. The improved agreement for the index  $\beta$  does suggest that the value obtained with single crystals may, in fact, have been affected by extinction.

## VI. SITE-DILUTED SAMPLES

A power-law fit to the temperature dependence of the Bragg intensity for the 5-at. % sample is shown in the log-log plot of Fig. 9. The least-squares fit was made without the lowest two points, but these points are consistent with the fit. The value of  $\beta=0.385 \pm 0.025$  is

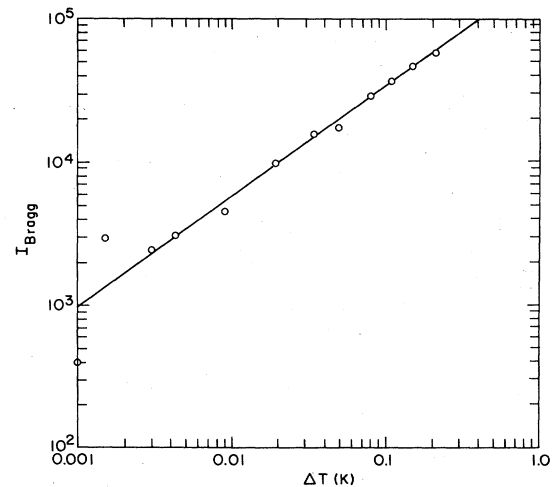


FIG. 9. Power-law fit of the temperature dependence of the magnetic Bragg intensity for the 5-at. % sample.

TABLE I. Calculated and observed critical parameters for pure DAG.

Quantity <sup>a</sup>	Theory <sup>b</sup>	Expt. DAG powder	Expt. DAG single crystal
$\beta$	0.325	$0.33 \pm 0.01$	$0.26 \pm 0.02$
$\nu$	0.634	$0.66 \pm 0.05$	$0.61 \pm 0.02$
$\nu'$	0.634	$0.64 \pm 0.05$	
$\gamma'$	1.24	$1.39 \pm 0.09$	
$F/F'$	2.0	$2.9 \pm 0.3$	

<sup>a</sup> $F$  and  $F'$  are amplitudes of the power laws for  $\kappa$  and  $\kappa'$ .

<sup>b</sup>J. L. LeGuillou and J. Zinn-Justin, Phys. Rev. B 21, 3976 (1980); for amplitude ratio see H. B. Tarko and M. E. Fisher, Phys. Rev. Lett. 31, 926 (1973).

somewhat higher than the theoretical value of 0.350 for the random Ising model, but considering the error estimate, is not seriously in disagreement.

While the staggered magnetization behaves normally, the critical scattering above  $T_N$  exhibits a highly anomalous variation with temperature. Far above  $T_N$ , as can be seen in Fig. 10, the temperature dependence of the inverse range parameters is qualitatively what one would expect it to be. At about 0.01 degrees above  $T_N$ , the value of  $\kappa$  drops precipitously to very low values. The values close to  $T_N$  seem to decrease with temperature but are experimentally almost indistinguishable from zero. It should be emphasized that throughout the temperature range of Fig. 10, the scattering is very well described by the powder average of a simple Lorentzian, and that furthermore, there is no evidence of Bragg scattering. The transition remains sharp, as can be seen in Figs. 3 and 4, with rounding less than 1 mK.

We can choose a temperature  $T_N^*$  ( $> T_N$ ) such that between  $T_N$  and  $T_N^*$ ,  $\kappa \sim 0$  and the sample exhibits essentially "infinite" staggered susceptibility, and above  $T_N^*$  the inverse range parameter is characterized by a power law with a reasonable exponent. Inspection of Fig. 10 suggests that  $T_N^*$  might be taken to be 2.418 K, which is about 9 mK or 9 times the estimated error in  $T_N$ , above

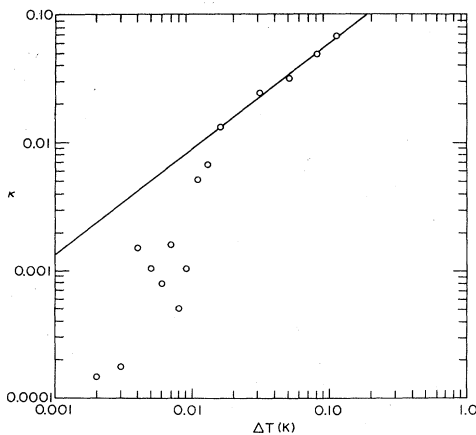


FIG. 10. Temperature dependence of the inverse range parameter  $\kappa$  in the 5-at. % sample. The straight line is a least-squares fit to the higher-temperature points only, and corresponds to  $\nu=0.82$ .

the critical point defined by the onset of Bragg scattering. With this choice of  $T_N^*$ , the power law for the remaining values of  $\kappa$  is characterized by a not unreasonable value of  $\nu$ , 0.646, as can be seen in Fig. 11. No error has been assigned to this value inasmuch as the choice of  $T_N^*$  is somewhat arbitrary.

The results for the 1-at. % sample are qualitatively similar to those for the 5-at. % sample. Once again  $\beta$  is normal and the critical scattering shows an "infinite susceptibility" range which in this case is approximately 5 mK wide. A summary of results for pure and diluted samples is given in Table II, together with pertinent theoretical estimates.

## VII. DISCUSSION

As can be seen from Table II, the values of  $\beta$  exhibit changes on dilution which are comparable to those predicted theoretically. The values of  $T_N$  decrease on dilution as one would expect, because of the decrease in the number of magnetic neighbors. Unlike the situation in  $\text{MnF}_2$  (Ref. 10) and  $\text{FeF}_2$  (Ref. 11) where dilution with Zn gives rise to an approximately linear dependence of  $T_N$  on concentration, the temperature dependence in the DAG-yttrium system shows marked curvature even over the restricted range studied. Perhaps this behavior is related to the complex interaction paths in DAG and the known importance of dipolar interactions in addition to exchange.

The progressive change in the size of the infinite susceptibility region with dilution supports the idea that the

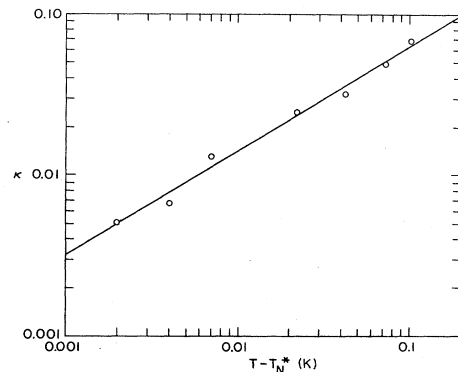


FIG. 11. Power-law fit of  $\kappa$  vs  $T - T_N^*$  for the 5-at. % sample, with  $T_N^* = T_N + 0.009$  K, as explained in the text.

TABLE II. Critical data for pure and diluted DAG.

Quantity	Ideal Ising (theor.)	Pure	1 at. %	5 at. %	Random Ising (theor.)
$\beta$	0.325 <sup>a</sup>	0.330±0.012	0.350±0.01	0.385±0.025	0.350 <sup>b</sup>
$T_N$		2.559, K	2.503 <sub>2</sub> K	2.409 K	
Range of infinite $\chi$ ( $T_N^* - T_N$ )		0	0.005 K	0.009 K	
$\nu$	0.634 <sup>a</sup>	0.663±0.05	0.73 <sup>d</sup>	0.65 <sup>d</sup>	0.70, <sup>b</sup> 0.68 <sup>c</sup>

<sup>a</sup>J.C. LeGuillou and J. Zinn-Justin, Phys. Rev. B 21, 3976 (1980).

<sup>b</sup>K. E. Newman and E. K. Riedel, Phys. Rev. B 25, 264 (1982).

<sup>c</sup>G. Jug, Phys. Rev. B 27, 609 (1983).

<sup>d</sup>Power law is based on  $T_N^*$ .

observations reported here represent a real physical phenomenon and not a spurious effect that might appear accidentally in one sample. This kind of behavior has in fact been predicted by Aharony and Pytte<sup>12</sup> and by Mukamel and Grinstein<sup>13</sup> for certain systems with spin dimensionality greater than 1, but has not as yet been observed.

Application of an external field above  $T_N$  should induce random fields in the diluted samples which might actually increase the size of the infinite susceptibility region by further inhibiting the development of long-range order. Experiments to check this point were carried out but were almost impossible to interpret for reasons which appear to be unrelated to the presence of impurities: In a field applied along the [110] scattering vector, the antiferromagnetic Bragg peak fails to exhibit a sharp transition, and shows, instead, a gradual decrease in intensity with respect to either increasing field or temperature, on entering the paramagnetic phase. This characteristic makes it impossible to study the critical scattering at the center of the scan where one would have sufficient sensitivity to study the effect of field on the correlation range. Persistence of the Bragg scattering has been observed before in studies<sup>14</sup> of single crystals of pure DAG. Prior to that it had been shown<sup>15</sup> that application of a field in the [111] direction of DAG generates an induced (nonrandom) stag-

gered field proportional to  $H_x H_y H_z$ , which destroys the second-order transition and gives rise to an S-shaped decay of intensity with increasing field. This induced staggered field would be expected to vanish if one component of the applied field were zero, as in the case of a field along [100] or [110]. However, subsequent measurements<sup>14</sup> on a pure single crystal, with field applied parallel to [110], indicate that the critical scattering reaches a peak as a function of field, with  $\kappa \sim 0$ , whereas the Bragg intensity persists above the field corresponding to this maximum. (The separation of Bragg and critical scattering is possible here because of the extreme sharpness of the Bragg reflection.) Clearly, another mechanism for the persistence of the antiferromagnetic Bragg peak is operative here, and probably in powders as well.

#### ACKNOWLEDGMENTS

We acknowledge the collaboration of W. Wolf in earlier studies leading up to the present investigation. We also thank A. Aharony, S. Coppersmith, V. J. Emery, D. Mukamel, A. Ramirez, and Y. Shapir for helpful discussions. This research was carried out at Brookhaven National Laboratory under Contract No. DE-AC02-76CH00016 with the U.S. Department of Energy and supported by its Division of Materials Sciences, Office of Basic Energy Sciences.

<sup>1</sup>A. B. Harris, J. Phys. C 7, 1671 (1974).

<sup>2</sup>A. B. Harris and T. C. Lubensky, Phys. Rev. Lett. 33, 1540 (1974); T. C. Lubensky, Phys. Rev. B 11, 3580 (1975); G. Grinstein and A. Luther, *ibid.* 13, 1329 (1976); D. E. Khmel'nitskii, Zh. Eksp. Teor. Fiz. 68, 1960 (1975) [Sov. Phys.—JETP 41, 981 (1976)]; C. Jayaprakash and H. J. Katz, Phys. Rev. B 16, 3987 (1977).

<sup>3</sup>K. E. Newman and E. K. Riedel, Phys. Rev. B 25, 264 (1982).

<sup>4</sup>G. M. Meyer and O. W. Dietrich, J. Phys. C 11, 1451 (1978).

<sup>5</sup>R. A. Cowley and K. Carneiro, J. Phys. C 13, 3281 (1980).

<sup>6</sup>R. A. Dunlap and A. M. Gottlieb, Phys. Rev. B 23, 6106 (1981).

<sup>7</sup>R. J. Birgeneau, R. A. Cowley, G. Shirane, H. Yoshizawa, D. P. Belanger, A. R. King, and V. Jaccarino, Phys. Rev. B 27, 6747 (1983).

<sup>8</sup>D. P. Landau, B. E. Keen, B. Schneider, and W. P. Wolf, Phys. Rev. B 3, 2310 (1971); W. P. Wolf, B. Schneider, D. P. Landau, and B. E. Keen, *ibid.* 4472 (1972).

<sup>9</sup>J. C. Norvell, W. P. Wolf, L. M. Corliss, J. M. Hastings, and R. Nathans, Phys. Rev. 186, 557 (1969); 186, 567 (1969).

<sup>10</sup>D. P. Belanger, F. Borsa, A. R. King, and V. Jaccarino, J. Magn. Magn. Mater. 15-18, 807 (1980).

<sup>11</sup>G. K. Wertheim, D. N. E. Buchanan, and H. J. Guggenheim, Phys. Rev. 152, 527 (1966).

<sup>12</sup>A. Aharony and E. Pytte, Phys. Rev. Lett. 45, 1583 (1980).

<sup>13</sup>D. Mukamel and G. Grinstein, Phys. Rev. B 25, 381 (1982).

<sup>14</sup>J. M. Hastings and L. M. Corliss (unpublished).

<sup>15</sup>M. Blume, L. M. Corliss, J. M. Hastings, and E. Schiller, Phys. Rev. Lett. 32, 544 (1974); R. Alben, M. Blume, L. M. Corliss, and J. M. Hastings, Phys. Rev. B 11, 295 (1975).